Measuring Matter Antimatter Asymmetries at the LHC
Third Year Lab Report

Euan Baldwin 10818421
Department of Physics and Astronomy, University of Manchester
(Experiment performed in collaboration with Luca Vicaria 10828724)
(Dated: December 15, 2023)

This report analyses the fundamental difference between the behaviour of matter and antimatter through the analysis of bottom meson decay data collected at the LHCb experiment. For the decay analysed, $B^{\pm} \rightarrow \pi^{+}\pi^{-}\pi^{\pm}$, a global matter-antimatter asymmetry of $0.058 \pm 0.004(\text{stat}) \pm 0.013(\text{syst}) \pm 0.007(\text{J}/\psi\text{K}^{\pm})$ is calculated. This result is evidence of an inclusive CP asymmetry in charmless three-body B decays. Additionally, a larger asymmetry of $0.276 \pm 0.014(\text{stat}) \pm 0.013(\text{syst}) \pm 0.007(\text{J}/\psi\text{K}^{\pm})$ is found in a region of the phase space.

1. INTRODUCTION

Until the 1960's it was assumed that the combination of charge conjugation symmetry (transformation of a particle into its antiparticle) and parity symmetry (transformation of spatial coordinates), known collectively as CP-symmetry, was a fundamental symmetry of the universe [1]. If CP-symmetry holds the Big Bang should have produced equal amounts of matter and antimatter, resulting in the annihilation of both and the universe being nothing more than leftover energy. Nevertheless a small proportion of matter remains today - around one in ten billion particles [2]. This imbalance is hypothesised to be due to the violation of CP-symmetry, as outlined by the Sakharov conditions [3]. These asymmetries are described in the standard model by the Cabibbo-Kobayashi-Maskawa quark-mixing matrix [4][5]. However they are not large enough to explain the magnitude of the matter antimatter imbalance we observe in the universe today and hence additional sources of CP violation must be found in or beyond the standard model [2].

One source of CP violation, direct CP violation, requires two interfering amplitudes with different weak and strong phases to be involved in the decay process [6]. Large CP violation effects have been observed in charmless two-body B-meson decays [7][8]. However, the source of the strong phase difference in these processes is not well understood, which limits the potential to use these measurements to search for physics beyond the standard model. One possible source of the required strong phase difference is from final-state hadron rescattering, which can occur between two or more decay channels with the same flavor quantum numbers, such as $B^{\pm} \rightarrow \pi^{+}\pi^{-}\pi^{\pm}$ and $B^{\pm} \rightarrow K^{+}K^{-}\pi^{\pm}$. This is known as compound CP violation [9] and this effect is what this report aims to investigate both globally and locally in regions of Dalitz plot phase space.

2. METHODOLOGY

2.1. Data Collection

The data used in this report was collected by the LHCb (Large Hadron Collider beauty) experiment at CERN in 2011. The LHC collided two beams of protons (pp) with an integrated luminosity of one fb^{-1} and a center of mass energy of seven TeV. These crossed in the LHCb detector at a rate of 15 MHz [10].

The LHCb, as shown in Figure 1, is a single-arm forward spectrometer, designed for the study of particles with a polar angle of 15 to 300 mrad, namely particles containing b or c quarks such as the B-meson.

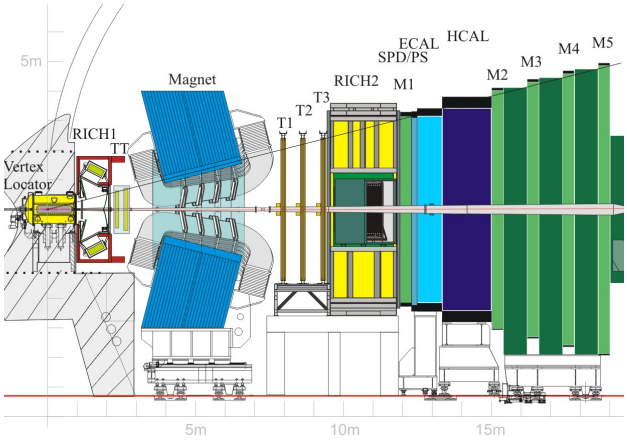

FIG. 1. LHCb detector view among the bending plane showing the vertex locator where the pp collision happens, the magnet, and the sub-detectors. Taken from [11].

Event selection is conducted via a dual-stage trigger mechanism, comprising a hardware phase and a subsequent software phase [12]. The hardware trigger relies on data from a calorimeter system and five muon stations, whereas the software trigger implements comprehensive event reconstruction. Further specifics on the individual sub-detectors are available in [11]. Initially, candidate events must satisfy the hardware trigger criteria, which selects particles exhibiting significant transverse energy. The software stage of the trigger then necessitates the presence of a two-, three-, or four-track secondary vertex characterised by a high cumulative transverse momentum, p_T, and a notable separation from the primary pp collision vertices. To ascertain the compatibility of secondary vertices with B hadron decay events, a multivariate algorithm is employed, as documented in [13].

2.2. Offline Data Selection

Offline selection criteria are then applied to select B-mesons and suppress the combinatorial background. These are detailed in Table I. Final-state kaons and pions are selected using particle identification information, provided by the two ring-imaging Cherenkov detectors. The optimal cuts, found via trial and error, are to eliminate particles based on a combination of their individual and multiplied probabilities. Additionally, event tracks are required to be incompatible with a muon. By making Dalitz plots, with axes being the squares of the invariant masses of two pairs of the two-body masses, $m^2_{low,\pi^+\pi^-}$ and $m^2_{high,\pi^+\pi^-}$, the intermediate resonances will be visible as bands on the Dalitz Plot. Spin zero (scalar) resonances will produce uniformly populated bands whereas spin one (vector) res-

Variable	Selection Cut
Individual pion probabilities, $P_i(\pi)$	> 0.1
Individual kaon probabilities, $P_i(\mathrm{K})$	< 0.9
Individual muon probabilities, $P_i(\mu^-)$	$= 0$
$P_1(\pi) * P_2(\pi) * P_3(\pi)$	> 0.7
$P_1(\mathrm{K}) * P_2(\mathrm{K}) * P_3(\mathrm{K})$	< 0.2
2-body mass assuming tracks are pions	$\neq 1.87 \pm 0.03$ GeV/c^2
Track Transverse Momentum (p_T)	> 0.1 GeV/c
Sum of p_T of Tracks	> 4.5 GeV/c
Track Momentum	> 1.5 GeV/c
B^+ mass assuming all tracks are K^+	> 5.05 GeV/c^2 < 6.30 GeV/c^2
Track Impact Parameter (IP) χ^2	> 1
Sum of IP χ^2 of Tracks	> 500
B^+ candidate vertex fit χ^2	< 12

TABLE I. Offline selection criteria for particle tracks. Modified from [14].

onances will show a minimum in the band. The analysis reveals two resonances: the first, located at 770 $\mathrm{MeV/c^2}$, aligns with the characteristics of the spin-zero rho meson [15]. The second resonance, observed as a uniformly populated band at 1870 $\mathrm{MeV/c^2}$, is consistent with the properties of the spin-half D_0 meson. Charm contributions are removed by excluding the regions of ± 30 $\mathrm{MeV/c^2}$ around the world average value of the D_0 mass, 1870 $\mathrm{MeV/c^2}$, in the two-body invariant masses [15].

2.3. *Calculating Asymmetries*

The raw CP-asymmetry, A_{raw}, is defined as

$$A_{raw} = \frac{N^- - N^+}{N^- + N^+} \tag{1}$$

where N^+ is the number of $B^+ \to \pi^+\pi^-\pi^+$ events observed and N^- the number for the corresponding $B^- \to \pi^+\pi^-\pi^-$ decay. The value of $N^\pm$ can be estimated by fitting the $B^\pm$ invariant mass distribution as a Gaussian to extract the signal event contribution from the exponentially distributed background.

The statistical uncertainty on the raw asymmetry is given by

$$\sigma_A = \sqrt{\frac{1 - A_{raw}^2}{N^- + N^+}} \tag{2}$$

where several assumptions are made, including that the asymmetry is a binomially distributed random variable (valid as for N^+ equals N^- there is zero asymmetry and $\sigma_A \to 0$) and that the efficiencies of $N^\pm$ are anti-correlated (valid as they sum to one).

CP violation arises from the interference between decays through different resonances, and hence the magnitude and sign of the CP violation may vary across a Dalitz plot. Hence, by plotting this phase space we can identify regions of significant asymmetry and re-calculate the localised CP asymmetry.

Systematic uncertainties, stemming from various factors, must be taken into account. The detector's lack of perfect symmetry, caused by either inherent features like unevenly arranged components or due to local faults, is a key consideration. Any local asymmetry in the detector, which might favour one side, is inverted when the magnetic field's polarity is changed. Therefore, to neutralise these asymmetries we average the results obtained from both magnetic field orientations weighted by the number of events in each data set.

Another source of systematic uncertainty arises from the fitting procedure. To address this, several valid fitting procedures are attempted, such as treating the background as linear or treating the signal as a Crystal Ball function [16]. The variation in results obtained from these different fitting approaches forms the basis for the systematic uncertainty which is then added in quadrature to the detector-related systematic uncertainty.

There is a further asymmetry arising from interactions of final-state particles with matter. This is accounted for using the well-understood reference mode of $B \to \mathrm{J}/\psi\mathrm{K}^\pm$. The CP asymmetry is hence expressed in terms of the raw asymmetry and a correction $A(\mathrm{J}/\psi\mathrm{K}^\pm)$

$$A = A_{raw} - A(\mathrm{J}/\psi\mathrm{K}^\pm) \tag{3}$$

where the world average value for this correction is $A(\mathrm{J}/\psi\mathrm{K}^\pm) = 0.001 \pm 0.007$ [15].

3. RESULTS

The post-cutting invariant mass spectra of the $B^\pm \to \pi^+\pi^-\pi^\pm$ are shown in Figure 2. As detailed in the methodology, the signal is modelled as a Gaussian, while the combinatorial background is treated as an exponential. We also see four-body B-meson decays at a lower mass, these are modelled as a Gaussian. The reduced chi-squared of these fits were always within the acceptable range of $0.5 < \chi^2_R < 2$. By splitting data into $B^+ \to \pi^+\pi^-\pi^+$ and $B^- \to \pi^+\pi^-\pi^-$ the global matter-antimatter asymmetry can be calculated using Equations 1 and 3 and its statistical uncertainty via Equation 2. This gives a value for global CP asymmetry of $A_{global} = 0.058 \pm 0.004$.

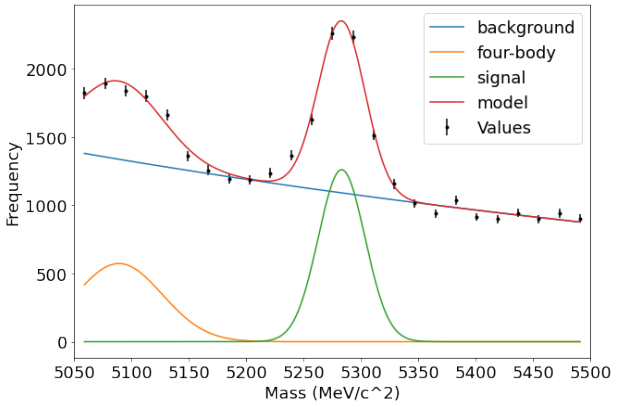

FIG. 2. Invariant mass spectra of $B^\pm \to \pi^+\pi^-\pi^\pm$. Background and four-body are modelled as Gaussian while the background is modelled as exponential, $\chi^2_R = 1.88$.

The magnet weighted CP asymmetry, when both magnetic polarity orientations are weighted by the number of events in each data set, is found to be $A_{mag} = 0.044 \pm 0.004$. By calculating the difference between this value and our previous global value we find this produces a systematic uncertainty of $A_{syst,mag} = 0.012$. Furthermore, the asymmetry when the background is treated as a linear function is found to be $A_{fit} = 0.052 \pm 0.004$, producing a systematic uncertainty of $A_{syst,fit} = 0.006$. Adding these in quadrature gives a total systematic uncertainty of $A_{syst} = 0.013$. Hence we find a global asymmetry of $A_{global} = 0.058 \pm 0.004 \pm 0.013 \pm 0.007$, where the first uncertainty is statistical, the second is the experimental systematic, and the third is due to the CP asymmetry of the $B \to \mathrm{J}/\psi\mathrm{K}^\pm$ reference mode [15].

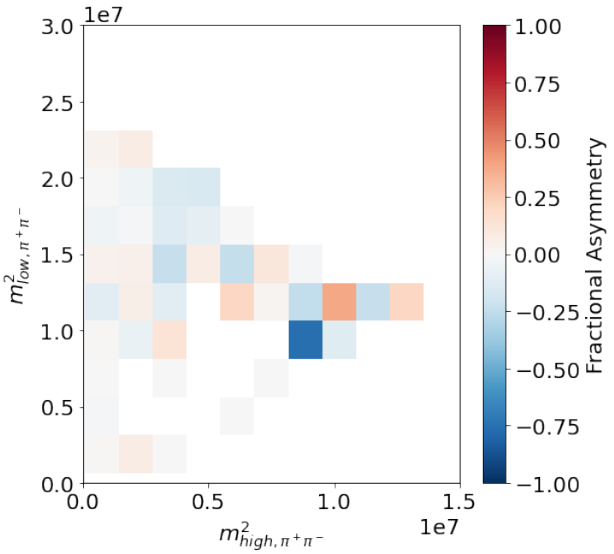

FIG. 3. Asymmetries of the number of events in bins of the Dalitz plot's localised phase space.

By plotting the Dalitz plot of the localised asymmetries, as shown in Figure 3, we selected out a region of the phase space with significant same sign asymmetry. We choose the region defined by the bounds ($m^2_{low,\pi^+\pi^-} < 0.8$) $\mathrm{MeV}^2/\mathrm{c}^4$ and ($1.6 < m^2_{high,\pi^+\pi^-} < 2.1$) $\mathrm{MeV}^2/\mathrm{c}^4$ which as can be seen in Figure 3 has a large positive asymmetry. This gives us a localised asymmetry of $A_{local} = 0.276 \pm 0.014 \pm 0.013 \pm 0.007$.

4. DISCUSSION

The significance of the inclusive charge asymmetries, calculated by dividing the central values by the sum in quadrature of the different uncertainties, are 3.8σ and 13.6σ for the global and local asymmetries respectively. We have therefore observed (3σ) global asymmetry and found evidence of (5σ) local asymmetry. These results therefore demonstrate a contributing source to compound CP violation via final-state hadron rescattering, and help to explain the matter antimatter imbalance in the universe.

The established literature value for global CP asymmetry, as reported by the LHCb collaboration [10], is $A_{global} = 0.117 \pm 0.021 \pm 0.009 \pm 0.007$, and $A_{local} = 0.584 \pm 0.082 \pm 0.027 \pm 0.007$. Our observed global asymmetry value falls within 3σ of the literature value, indicating consistency. However, there is a notable discrepancy in our observed local asymmetry value. This can be attributed to the LHCb collaboration's methodology of employing bins weighted by particle count in their Dalitz plot analysis. This approach facilitates a more precise identification of regions with maximal CP asymmetry. Hence, to enhance the efficacy of local asymmetry detection in future investigations, we could adopt a similar strategy of utilising weighted bins.

The experimental methodology could also have been further expanded to include a broader spectrum of fitting functions, specifically incorporating the ARGUS function for modeling signal events and the Cruijff function for the lower mass four-body background events [10]. These functions have been effectively employed by the LHCb collaboration in their measurements of CP violation, suggesting their potential to enhance the optimisation of the fitting model in this study.

Finally, an improved approach for the mass selection cuts could have been used. For example, the implementation of an algorithm designed to identify the optimal mass cuts. This could have been achieved through the deployment of an auto-encoder, trained specifically on prevalent background events, thereby maximising the signal-to-background event ratio.

5. CONCLUSIONS

We have found evidence (3.8σ) of positive inclusive CP asymmetries in the $B^\pm \to \pi^+\pi^-\pi^\pm$ decay of magnitude $0.058 \pm 0.004(\mathrm{stat}) \pm 0.013(\mathrm{syst}) \pm 0.007(\mathrm{J}/\psi\mathrm{K}^\pm)$, thereby helping to explain the matter antimatter imbalance in the universe. This result is consistent with measurements from the LHCb collaboration [10]. These charge asymmetries are not uniformly distributed in the phase space and a large positive asymmetry (13.6σ) is measured in the low $m^2_{low,\pi^+\pi^-}$ and high $m^2_{high,\pi^+\pi^-}$ phase-space region with magnitude $0.276 \pm 0.014(\mathrm{stat}) \pm 0.013(\mathrm{syst}) \pm 0.007(\mathrm{J}/\psi\mathrm{K}^\pm)$. Several improvements to the experimental techniques are suggested, including using weighted Dalitz plot bins and other viable fitting functions. The evidence presented here for CP violation in $B^\pm \to \pi^+\pi^-\pi^\pm$ indicates new mechanisms for CP asymmetries which should be incorporated in models for future amplitude analyses of charmless three-body B decays.

[1] J. H. Christenson, J. W. Cronin, V. L. Fitch, and R. Turlay, Physical Review Letters **13**, 138 (1964).
[2] L. Canetti, M. Drewes, and M. Shaposhnikov, New Journal of Physics **14**, 095012 (2012).
[3] A. D. Sakharov, Pisma Zh. Eksp. Teor. Fiz. **5**, 32 (1967).
[4] N. Cabibbo, Phys. Rev. Lett. **10**, 531 (1963).
[5] M. Kobayashi and T. Maskawa, Progress of theoretical physics **49**, 652 (1973).
[6] M. Bander, D. Silverman, and A. Soni, Phys. Rev. Lett. **43**, 242 (1979).
[7] K. Abe *et al.*, Physical Review Letters **87**, 10.1103/physrevlett.87.091802 (2001).
[8] B. Aubert *et al.*, Physical Review Letters **86**, 2515–2522 (2001).
[9] H.-Y. Cheng, C.-K. Chua, and A. Soni, Phys. Rev. D **71**, 014030 (2005).
[10] R. Aaij *et al.*, Physical Review Letters **112**, 10.1103/physrevlett.112.011801 (2014).
[11] The European Organization for Nuclear Research, The LHCb Detector (2008), https://lhcb-outreach.web.cern.ch.
[12] R. Aaij *et al.*, Journal of Instrumentation **8** (4), P04022–P04022.
[13] V. V. Gligorov and M. Williams, Journal of Instrumentation **8** (02), P02013–P02013.
[14] M. Gersabeck and C. Parkes, Measuring Matter Antimatter Asymmetries at the Large Hadron Collider (2023), Lab script.
[15] J. Beringer *et al.* (Particle Data Group), Phys. Rev. D **86**, 010001 (2012).
[16] J. E. Gaiser, *Charmonium Spectroscopy from Radiative Decays of the J/Psi and Psi-Prime*, Ph.D. thesis, Stanford University (1982).